NASA TECHNICAL NOTE

NASA TN D-2884

NASA TN D-2884

DEVELOPMENT OF A HEMISPHERICAL METAL DIAPHRAGM FOR SINGLE-CYCLE LIQUID-METAL POSITIVE EXPULSION SYSTEMS

by Sol Gorland

Lewis Research Center

Cleveland, Ohio

NATIONAL AERONAUTICS AND SPACE ADMINISTRATION • WASHINGTON, D. C. • JUNE 1965

NASA TN D-2884

DEVELOPMENT OF A HEMISPHERICAL METAL DIAPHRAGM FOR SINGLE-CYCLE LIQUID-METAL POSITIVE EXPULSION SYSTEMS

By Sol Gorland

Lewis Research Center
Cleveland, Ohio

NATIONAL AERONAUTICS AND SPACE ADMINISTRATION

For sale by the Clearinghouse for Federal Scientific and Technical Information
Springfield, Virginia 22151 – Price $1.00

DEVELOPMENT OF A HEMISPHERICAL METAL DIAPHRAGM FOR SINGLE-CYCLE LIQUID-METAL POSITIVE EXPULSION SYSTEMS

by Sol Gorland

Lewis Research Center

26652

SUMMARY

This report presents experimental results pertaining to the design and development of a metallic expulsion diaphragm for single-cycle positive expulsion of high-temperature liquid in an agravity condition. The diaphragms were made from type 304 stainless steel having a wall thickness of 10 or 16 mils. Tests were conducted in a 22-inch-diameter transparent lucite sphere in order to observe the diaphragm during the expulsion cycle. For simplicity, water was used as the working fluid, both pressurant and expellant.

Greater than 98 percent expulsion without failure was obtained only with a diaphragm configuration less than a complete hemisphere. A diaphragm with a 1/2-inch equatorial segment removed from a 22-inch-diameter hemisphere successfully expelled over 98 percent of the enclosed liquid. Diaphragms slightly larger than complete hemispheres could only obtain between 60 and 82 percent expulsion before failure. It appears that metallic diaphragms without a method of controlling random deformation cannot go through more than one complete expulsion cycle without failure.

Author

INTRODUCTION

As part of an overall program to provide a single-cycle positive expulsion device for a liquid-metal flow system, a metal-diaphragm type of expulsion unit was investigated. The expulsion device was specifically intended for use in a heat-transfer study, requiring the storage and expulsion of fluids at temperatures in excess of 500° F under zero-gravity conditions.

Methods of transferring fluids during agravity conditions are a major design problem. One solution is the use of a positive expulsion device. Space missions and maneuvers requiring positive expulsion in a zero-gravity environment are described in reference 1. A thorough survey of expulsion techniques for liquids stored at or near room temperature was made in reference 2. References 3 and 4 investigated the use of collapsing bladder-type expulsion devices for cryogenics. A literature search did not indicate any published information relative to the use of a metal diaphragm for the expulsion of high-temperature liquid metals.

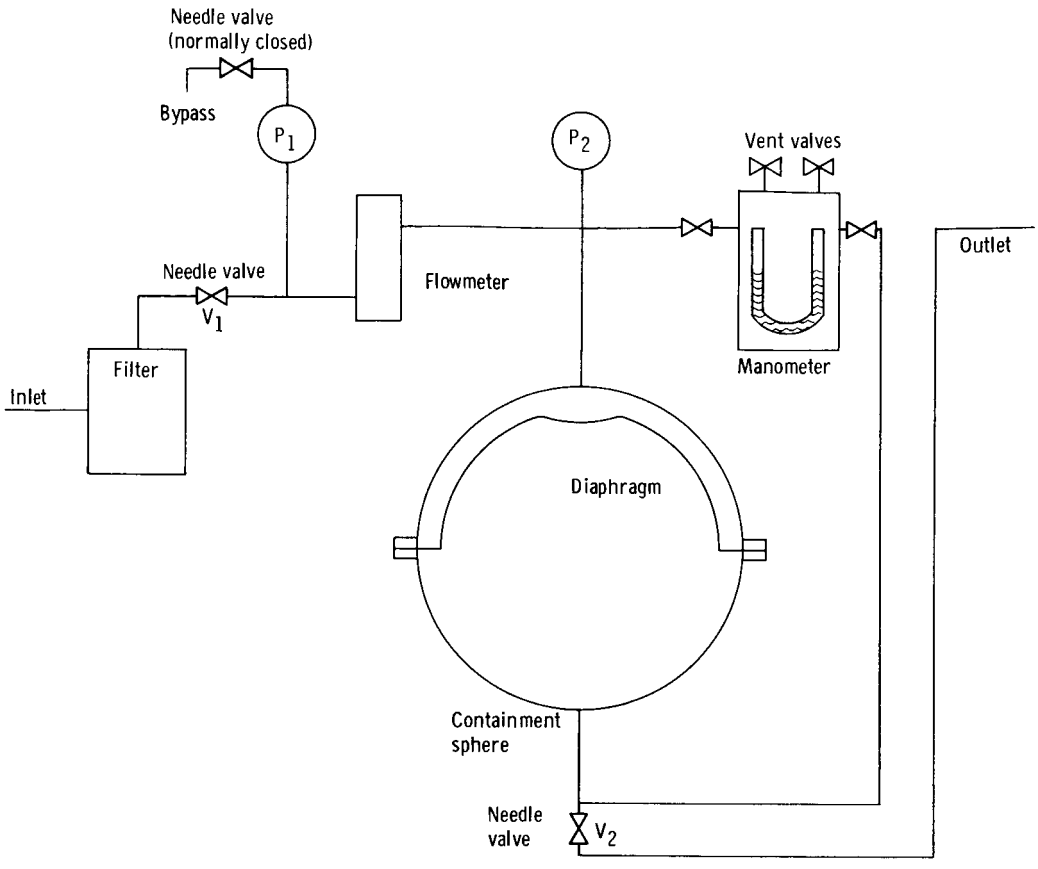

Figure 1. - Schematic diagram of flow system for expulsion diaphram tester.

The purpose of this program was to investigate at room temperature the behavior of a metal diaphragm expulsion device intended for single-cycle operation with a percent expulsion greater than 95 percent. The investigation was performed with corrosion- and radiation-resistant expulsion diaphragms that could be used with high-temperature liquid metals.

Desirable qualities of an expulsion unit for space applications are lightweight, reliability, simplicity, and high volumetric and expulsion efficiency. Volumetric efficiency is the total volume minus the ullage of the container, while expulsion efficiency is the percent enclosed by the diaphragm that is possible to expel. The expulsion device tested consisted of a transparent 22-inch-diameter simulated containment tank and a prototype hemispherical stainless-steel diaphragm designed to store and expel fluids at temperatures above 500° F. Actual testing was performed using water at room temperature with flow rates ranging from 150 to 500 pounds per hour and for pressure differentials across the diaphragm in the order of 1 to 2 pounds per square inch.

APPARATUS

A schematic of the test apparatus is shown in figure 1. The expulsion system consisted of a spherical storage container, an expulsion diaphragm, a pressurization system, and the required valves and gages. Figure 2 is a photograph of the experimental apparatus.

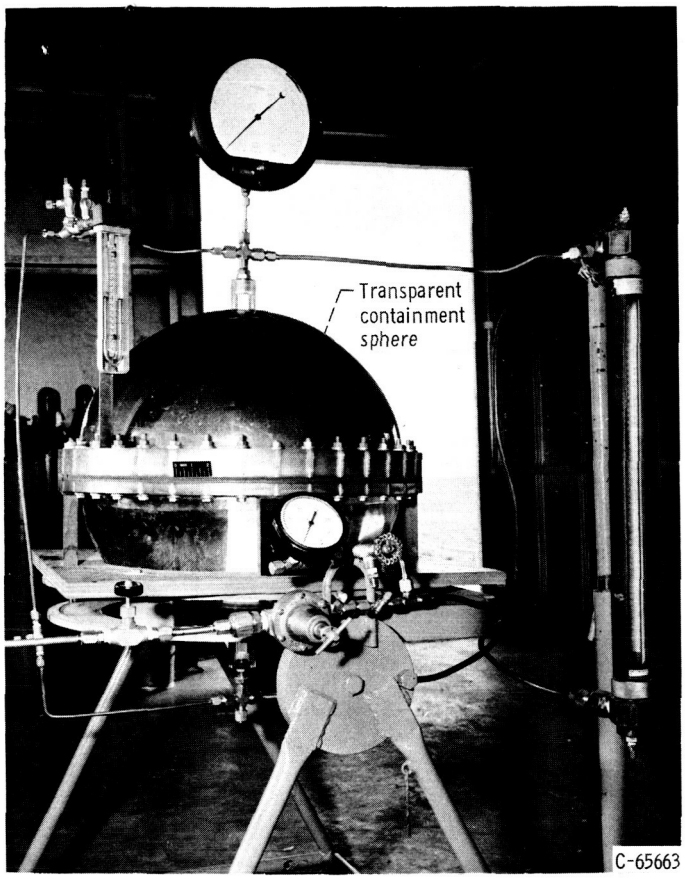

Figure 2. - Expulsion apparatus for experimental test of expulsion diaphragm.

Containment Sphere

The containment sphere consisted of two 22-inch-diameter hemispheres made from transparent lucite. Lucite flanges were attached to each hemisphere so that when bolted together the inside surface formed two 22-inch-diameter hemispheres separated by a 1-inch cylindrical section. Rubber gaskets were used between the flanges to act as both seals and spacers. Each hemisphere had a 4-inch-diameter hole at its pole to which lucite fittings were attached so that flow lines could be connected. The containment sphere was mounted on a platform attached to a stationary stand. The platform could be rotated 360° about a horizontal axis; this rotating feature facilitated the filling of the container, which will be discussed in the section Test Procedure.

Expulsion Diaphragm

The diaphragm was a separate assembly and was placed in the containment sphere just prior to testing. Each diaphragm was equipped with a mounting flange that was clamped between two rubber gaskets and held by the force of the flange bolts of the containment sphere. The material selected for the diaphragm was AISI 304 stainless steel. Fabrication of the diaphragm consisted of hydroforming 0.016- or 0.010-inch-thick stainless-steel sheet into 22-inch-diameter hemispheres with an additional 1-inch cylindrical section and an integral 1-inch flange around the edge. Heat treatment at 1400° F followed to anneal the hemispheres and remove residual stresses. An 8-inch-diameter indentation was made in the dome of the hemisphere to reduce the pressure necessary to start expulsion. Three diaphragm configurations were tested.

Configuration A

Figure 3 shows a sketch of the unmodified diaphragm, hereafter referred to as configuration A. Five configuration A diaphragms were fabricated; four were 0.016 inch thick, and one was 0.010 inch thick.

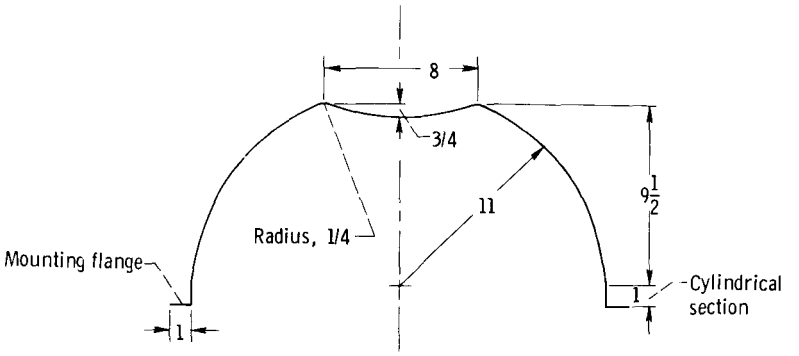

Figure 3. - Unmodified diaphragm. Configuration A. (All dimensions in inches.)

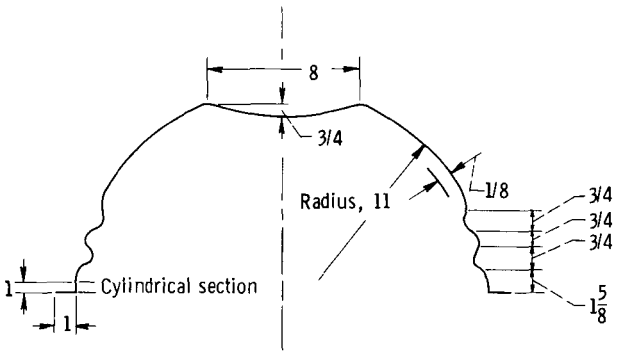

Figure 4. - Convoluted diaphragm. Configuration B. (All dimensions in inches.)

Configuration B

Configuration B consisted of a diaphragm containing a pair of corrugations that were spun onto the surface to allow easier rolling of the metal during expulsion as shown in figure 4. One 0.010-inch-thick configuration B diaphragm was fabricated.

Configuration C

Configuration C was essentially another modification of configuration A. It consisted of removing the 1-inch cylindrical section and 1/2-inch of the hemispherical section of the diaphragm as shown in figure 5(a). A new 1-inch-wide flange was then welded to the original material (to replace the integral flange of configurations A and B) so that the diaphragm could be clamped in the containment sphere. The flange was silver soldered to waterproof the joint as seen in figure 5(b). Configuration C was slightly less than a hemisphere and is actually a "segment" of configuration A. Two 0.016-inch-thick configuration C diaphragms were fabricated. Figure 5 shows a photograph of a configuration C diaphragm. Although configurations A and B were slightly different, figure 5(b) is typical of the diaphragms and clearly shows the polar indentation common to all.

Instrumentation

Instrumentation consisted of two pressure gages, a mercury manometer and a flowmeter as shown on the schematic of the experimental system in figure 1. A 60-pound-per-square-inch, $3\frac{1}{2}$-inch dial-face Bourdon gage (P_1) was used to measure the pressure of the incoming water (the pressurization system would be

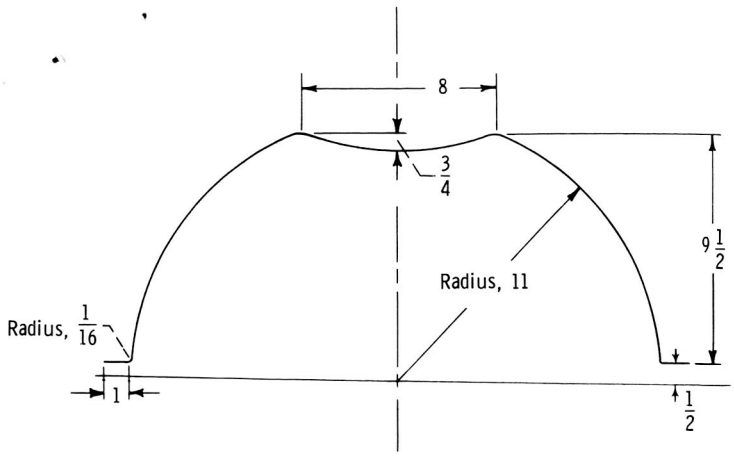

(a) Schematic. (All dimensions in inches.)

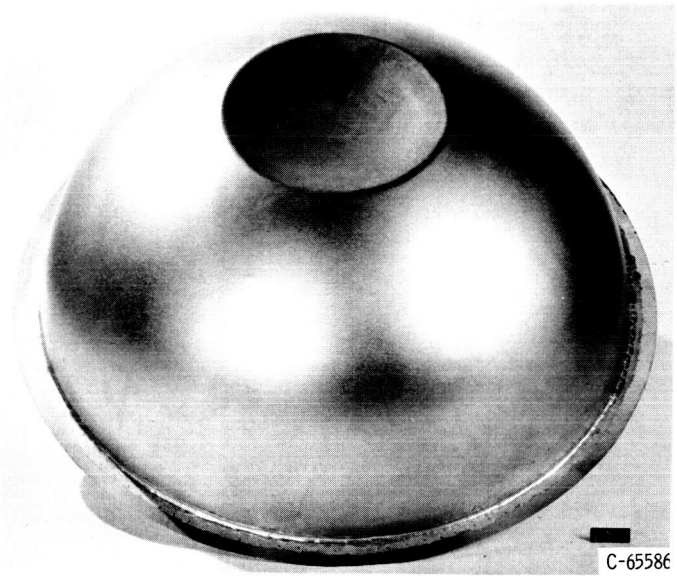

(b) Photograph.

Figure 5. - Final segmented hemispherical diaphragm. Configuration C.

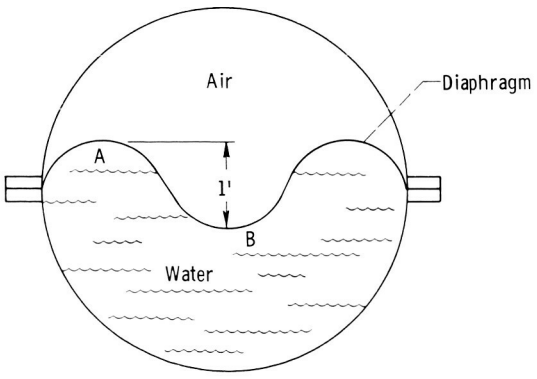

Figure 6. - Illustration of diaphragm deformation with air as pressurizing medium and water as expulsion medium.

gas in a flight system); a 15-pound-per-square-inch, 12-inch dial-face Heise gage (P_2) with scale increments of 0.05 pound per square inch and and accuracy of 1/2 percent, was used to measure the applied pressure on the diaphragm; the U-tube mercury manometer with scale increments of 1 millimeter measured the pressure differential across the diaphragm, each leg was open to water pressure on opposite sides of the diaphragm; a rotameter with an accuracy of ±5 pounds per hour was used to measure the flow of the pressurizing water.

Flow System

The pressurization system as well as the test fluid was provided by city water lines capable of 60 pounds per square inch. Air had been considered as a pressurizing agent, to better simulate actual use, but this was decided against because of the unequal pressure forces on the expulsion side of the diaphragm resulting from the hydraulic head. Figure 6 illustrates that, with air as the pressurizing medium, the force at A would be less than at B because of the hydraulic head difference. Therefore, to simulate zero gravity, the same fluid was used as both the pressurizing medium and the expulsion fluid. This is not necessary in actual flight operation, and a gas pressurization system would be used.

A siphoning effect will occur if the inlet and outlet flow lines are at different levels. The gravity head

was eliminated so that "true" flow and pressure readings would be obtained. This was accomplished by placing the gages and flow lines at the same elevation. Flow passages were kept short to minimize line pressure drop.

Test Procedure

Preparation for a test started with clamping a diaphragm into the containment sphere such that the diaphragm was on the lower half of the sphere. The sphere was then filled with water on the expulsion side of the diaphragm with care taken to eliminate air pockets. A valve was then attached to the expulsion side of the system, and the container was rotated 180° on the test stand so the expulsion diaphragm was now on the upper half of the sphere. The sphere was then filled on the pressurant side of the diaphragm using a graduated cylinder to measure the amount of water between the diaphragm and the containment sphere. An assembly consisting of the Heise gage and flow lines was then attached to the lucite fitting on the top pole of the sphere. The mercury manometer and rotameter were connected to the system, and the flow lines were filled from the city water line. Air entrapped in the lines was removed through the bypass line needle valve. The Heise gage was mechanically zeroed, and atmospheric vent valves were used to bleed air from the manometer legs.

Referring to figure 1 (p. 2), with no pressure on the system, the outlet valve on the containment sphere (V_2) was fully opened so that flow would not be restricted. The throttling needle valve (V_1) was opened to allow flow and set the system pressure. For most of the tests the initial flow established by setting V_1 was not changed. A floating-disc-type rotameter measured the flow rate into the lucite containment sphere. The static line pressure is indicated by P_1, and the applied pressure on the diaphragm is indicated by P_2. Tubing from the inlet and outlet of the containment sphere was connected to a manometer that measured the pressure differential across the diaphragm. At the end of a test, V_1 was shut to stop the flow. Photographs were taken of the expulsion diaphragms during the tests.

To determine the amount of water expelled, the diaphragm was removed; and, if it had leaked, the hole was soldered. The diaphragm was then replaced in the containment sphere, and the quantity of water remaining on the expulsion side of the diaphragm, between the diaphragm and containment sphere, was measured with a graduated cylinder. The percent expulsion of the diaphragm was found by: (1) calculating the total quantity of water enclosed by twice the volume of the diaphragm configuration minus the 8-inch-diameter indentation in the dome of the hemispheres; (2) subtracting the amount of water between the container and the diaphragm on the pressurant side of the diaphragm before expulsion minus the 8-inch-diameter indentation volume, from the quantity of water remaining between the container and the diaphragm on the expulsion side of the diaphragm after expulsion; and (3) dividing the second quantity by the first, multiplying by 100, and subtracting from 100 percent.

TABLE I. - DIAPHRAGM TYPE AND TEST RESULTS

Test number	Diaphragm thickness, in.	Expulsion, percent	Maximum applied starting pressure, psi	Flow rate, lb/hr	Configuration
1	0.016	~70	4	190	A
2	.016	76.5	---	220 to 225	A
3	.016	63.4	~2	295 to 375	A
4	.010	60.2	2.75	205 to 235	B
5	.010	68.5	2.80	180 to 210	A
6	.016	82.1	3.75	180 to 215	A
7	.016	95.6	4.15	350 to 376	C
8	.016	98.3	~9 (3.5 when reversed)	490 to 502	C

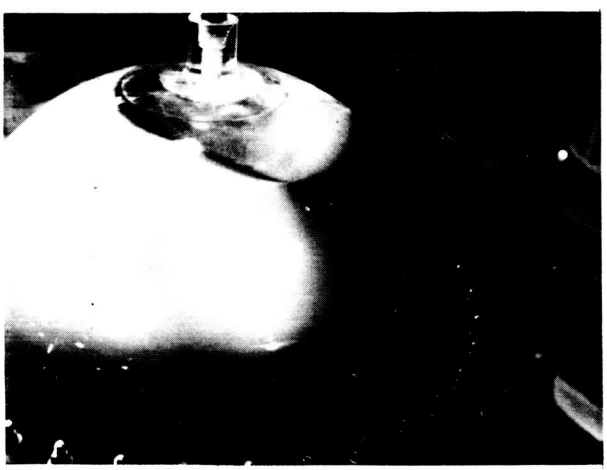

(a) Initial deformation showing assymetry (2 percent expulsion).

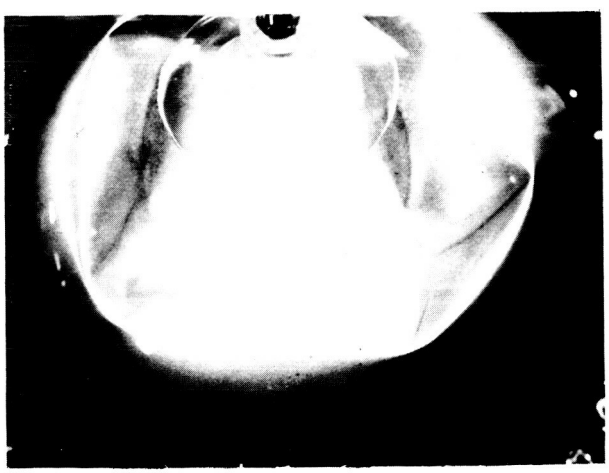

(b) Sharp-edged cornering (5 percent expulsion).

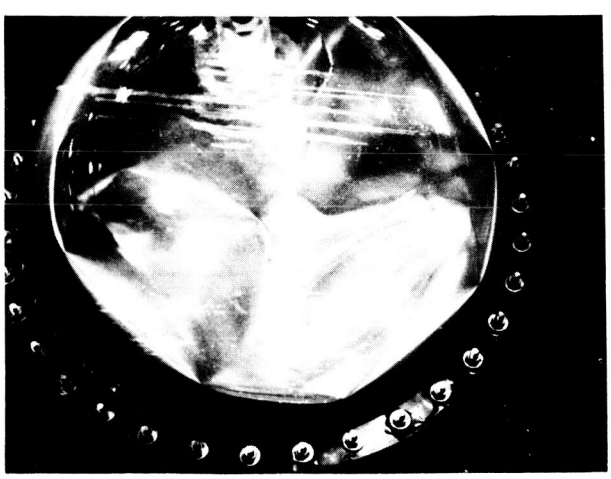

(c) Pyramid-type deformation (15 percent expulsion).

(d) Pyramid-type deformation closeup (15 percent expulsion).

Figure 7. - Progressive deformation of diaphragm during expulsion cycle. Configuration A; test 1, 0.016-inch-thick diaphragm; flow rate, ~190 pounds per hour.

RESULTS

Test 1, Configuration A, 0.016-Inch Wall Thickness

The first expulsion test was run as a shakedown for the experimental procedure and equipment. The flow rate as shown in table I was 190 pounds per hour. Deformation of the diaphragm began at an applied pressure of approximately 4 pounds per square inch. As shown in figures 7(a) and (e), deformation was unsymmetrical. A cornering effect started almost immediately, as seen in figure 7(b), but it did not seem to hinder deformation. Deformation took the form of a triangular pyramid-type deflection shown in figures 7(c) and (d). As the diaphragm neared the cylindrical section at the flange area, a double-fold-type deformation developed, which was typical of all the diaphragms tested. This is seen in figure 8 at a percent expulsion of approximately 60 percent. At approximately 65 percent expulsion, recycling was attempted to test the cycle capability of the diaphragm. Immediately, a torsional-type deformation developed (fig. 7(f)), similar to the twisting of a roll of paper. If recycling had continued, failure of the diaphragm would have occurred because of the severe twisting action, so the direction of expulsion was again reversed until approximately 85 percent of the original volume was displaced. The diaphragm developed a leak at approximately 70 percent expulsion, but since this was a shakedown run it was decided to continue the test beyond initial failure to study the deformation process. Upon removal, the diaphragm was found to have torn at one of the double folds. Figure 9 shows the first diaphragm after removal from the containment sphere; the tear at the double fold is circled.

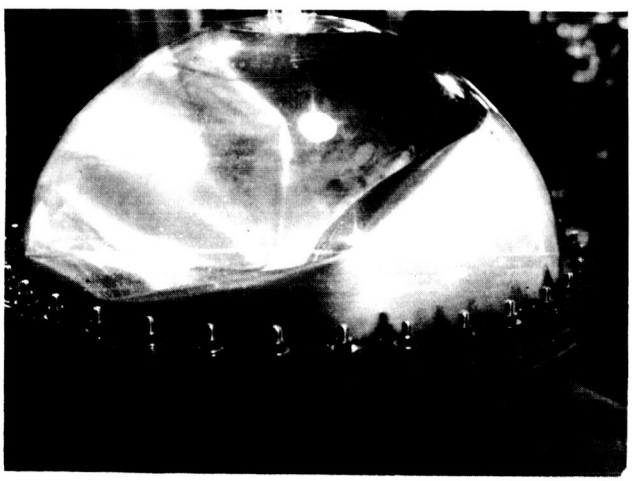

(e) Assymmetry of deformation (25 percent expulsion).

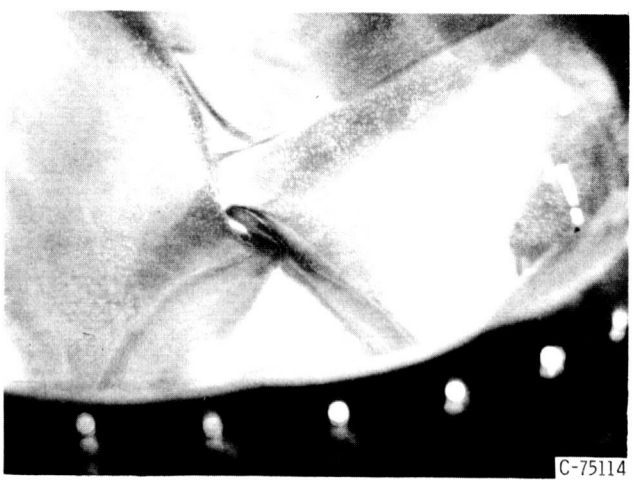

(f) Three corner fold as a result of torsional deformation (65 percent expulsion).

Figure 7. - Concluded.

Test 2, Configuration A, 0.016-Inch Wall Thickness

The second expulsion test repeated test 1 at a higher flow rate. An attempt was made to take motion pictures (1 frame/sec) of the entire test to see if the cause of the cornering and double folding could be determined; however, a complication developed. A dye (Azo Rubin) was added to the water on the pressurant side of the diaphragm during the

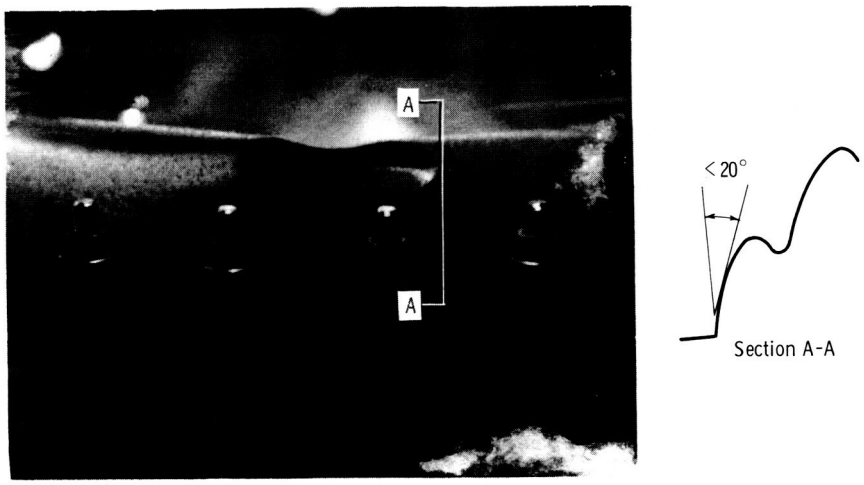

(a) Double fold in diaphragm.

(b) Closeup of double fold.

Figure 8. - Typical double fold. Configuration A, test 1; 0.016-inch-thick diaphragm (60 percent expulsion).

filling operation to check for tears in the diaphragm, but the dye mixture was too dark for the pictures to have good contrast. Deformation proceeded much as in the previous test.

Failure occurred, as previously, at a double fold. The dye made it possible to determine the moment of failure, so that the flow could be stopped, but a more dilute dye was necessary for photographic purposes. As shown in table I, the percent expulsion of the second diaphragm at the time of failure was 76.5 percent.

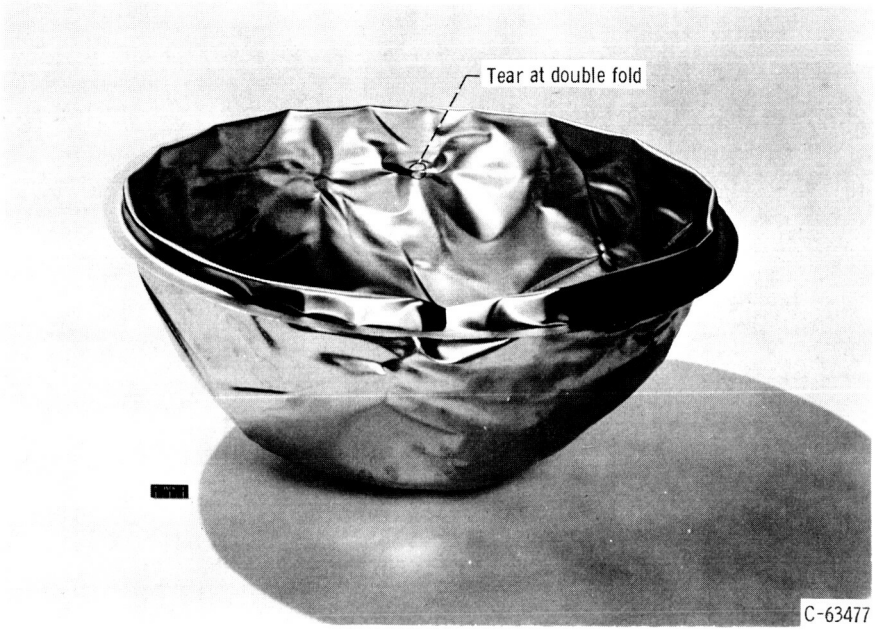

Figure 9. - Diaphragm configuration A at end of test 1 (85 percent total expulsion tear occurred at 70 percent expulsion).

Test 3, Configuration A, 0.016-Inch Wall Thickness

The third expulsion test again attempted to get motion pictures and also run the test at a higher flow rate. Failure again occurred at a double fold, the formation of which was similar to that for the other lower flow rates. The test was stopped when a hole developed in the diaphragm at an expulsion of 63.4 percent. Failure occurred earlier in the expulsion cycle than previous tests at lower flow rates. Films of this test clearly showed the method of deformation and the double fold phenomenon, which caused failure. These films aided in the visual analysis of the problem of diaphragm failure.

Test 4, Configuration B, 0.010-Inch Wall Thickness

In the fourth expulsion test, a 0.010-inch-thick hemisphere using configuration B (see fig. 4, p. 4) was tested. It was felt that the combination of the thinner material and the built-in convolutions would control the buckling and allow easier rolling of the metal thus possibly eliminating the double-fold-type deformation occurring at the cylindrical section of the diaphragm.

Flow was set so that comparison with test 2 would help determine the effects of the corrugations Failure occurred at approximately 60.2 percent expulsion. This is much below the 76.5 percent expulsion of test 2.

The corrugated hemisphere initially deformed very uniformly as shown in figure 10(a). It then began to deform on one side until the first or upper corrugation was reached. As seen in figure 10(b), it appeared that the material would easily roll over the corrugation, but cornering occurred in the corrugated area (fig. 10(c)). Columns formed in the corrugated areas (fig. 10(d))

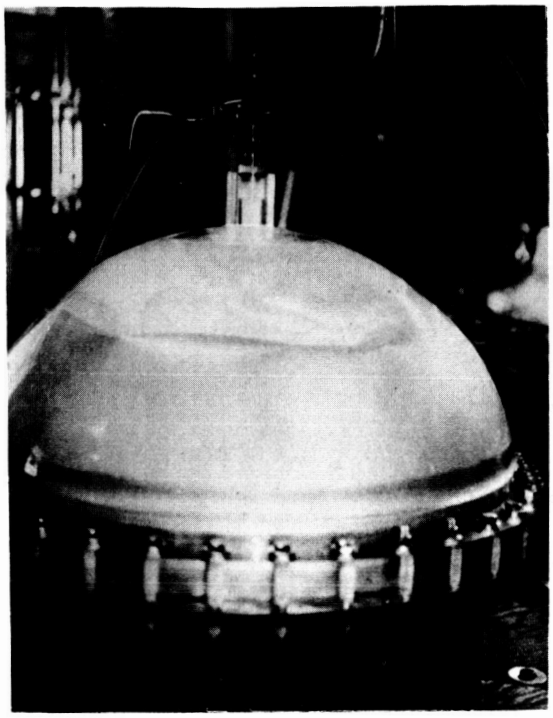

(a) Initial deformation of corrugated diaphragm (5 percent expulsion).

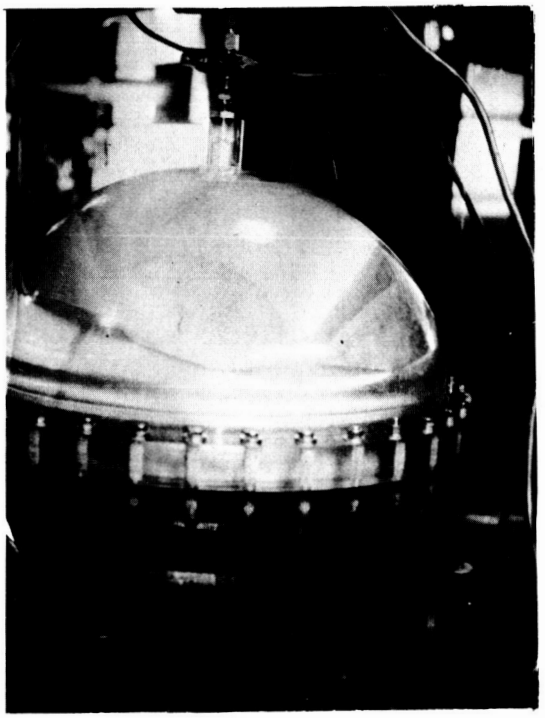

(b) Deformation nearing first corrugation (25 percent expulsion).

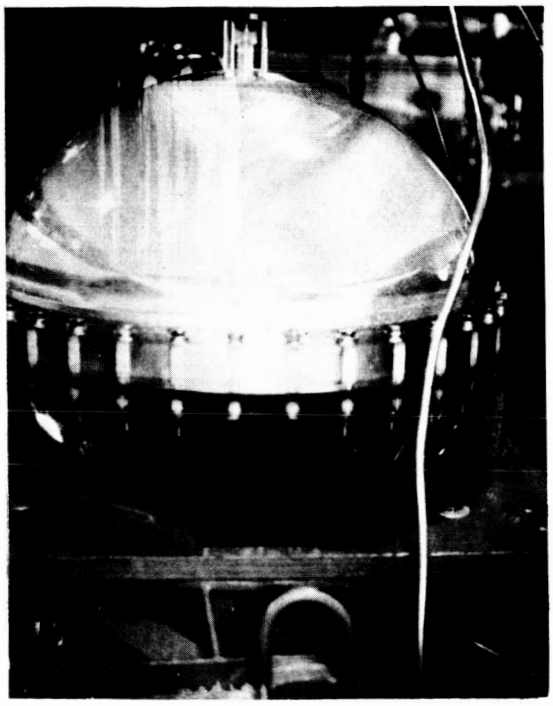

(c) Cornering effect in first corrugation (35 percent expulsion).

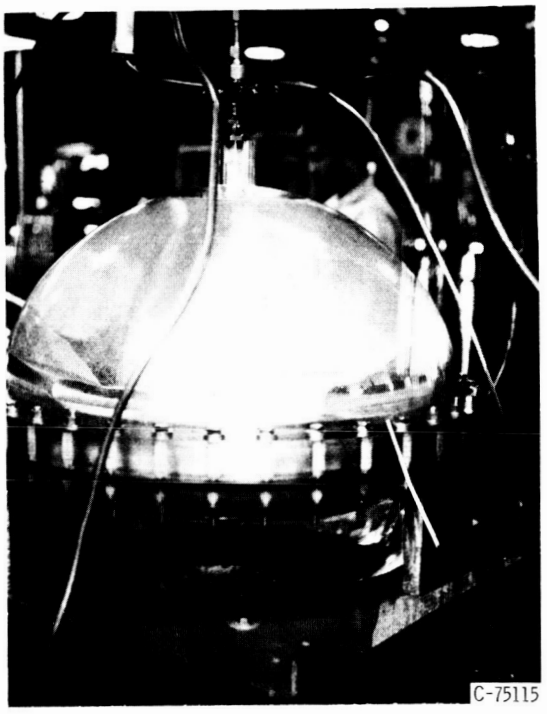

(d) Column formation in first corrugation (50 percent expulsion).

Figure 10. - Progressive deformation of diaphragm. Configuration B; test 4; 0.010-inch-thick diaphragm; flow rate, 205 to 235 pounds per hour.

supporting the hemisphere on that side until deformation was symmetrical. The second corrugation then became the starting point for the double fold phenomenon seen in figure 10(d). When this condition was attained, nearly the entire surface within the first corrugation seemed to double fold at once. Six double folds occurred almost simultaneously, all of which were larger than in the previous hemispheres. Three of these double folds produced tears at the failure point of 60.2 percent expulsion.

Test 5, Configuration A, 0.010-Inch Wall Thickness

The fifth expulsion test attempted to determine if either or both wall thickness and convolutions caused the premature failure of the corrugated diaphragm. The fifth diaphragm was an 0.010-inch wall hemisphere of configuration A. It was tested at a flow rate of 180 to 210 pounds per hour. Approximately 68.5 percent expulsion was achieved at failure. The diaphragms used in tests 4 and 5 had a lower total expulsion at failure than other diaphragms tested at a similar flow rate (tests 1 and 2). Both the material thickness and the corrugations seemed to be responsible. It appeared that the convolutions in diaphragm configuration B of test 4 gave the double fold phenomenon a place to form, causing an earlier failure than for type A diaphragms. The reason for eariler failure of the thinner material seemed to be associated with the mode of failure. Double folding was not as pronounced in the 0.010-inch-thick type A diaphragm (test 5) as for the 0.016-inch-thick type A diaphragm of tests 1, 2, and 3. Where the thinner material cornered, failure occurred by tearing rather than double folding as in previous tests. The 0.010-inch-thick material appeared to form sharper corners than the 0.016-inch material, resulting in higher local stresses thus causing tears earlier in the expulsion cycle.

Test 6, Configuration A, 0.016-Inch Wall Thickness

The sixth expulsion test was performed to obtain more data using an 0.016-inch-thick diaphragm of configuration A at a flow rate of 180 to 215 pounds per hour. An expulsion of 82.1 percent was obtained at failure.

Test 7, Configuration C, 0.016-Inch Wall Thickness

Observation of the previously tested units during the expulsion cycle and study of the slow motion films led to the decision to fabricate a diaphragm of configuration C. In the previous tests, it was observed that failure occurred at sharp bends (bend radius of ~0) formed in the 1-inch cylindrical section or in the section of the diaphragm whose tangent was nearly parallel to the direction of motion. With the removal of these sections, easier rolling of the metal in the flange area, due to the larger bend radius, could eliminate failure caused by the double folding effect.

The seventh expulsion test used a 0.016-inch-thick diaphragm of configuration C with the operating procedure remaining the same as previously. Dye was used to check for leaks. Flow was set at a moderately high level (375 lb/hr)

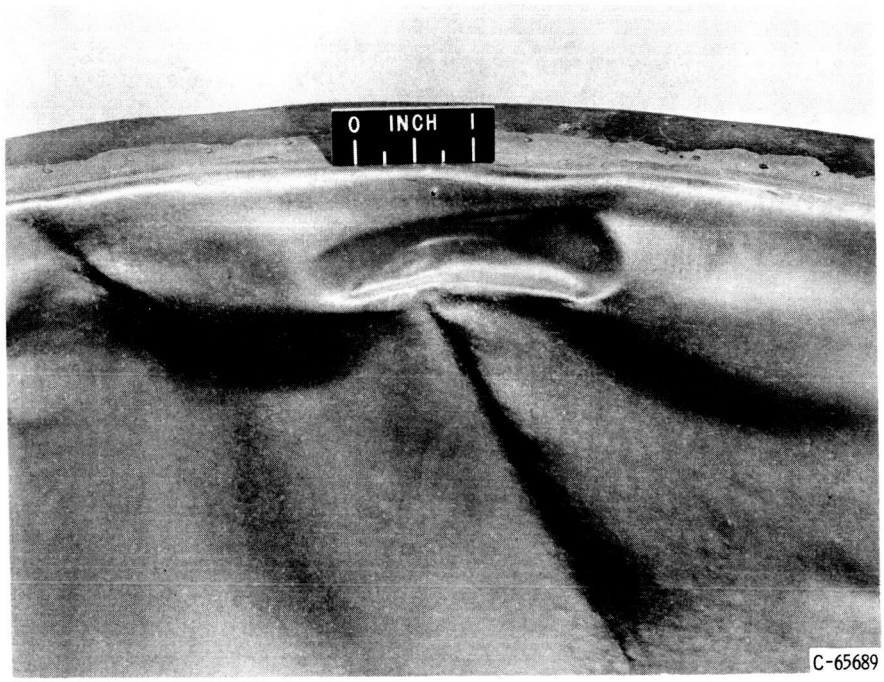

Figure 11. - Fully formed double fold in diaphragm configuration C after completion of expulsion cycle, 0.016-inch-thick diaphragm (95 percent expulsion, test 7).

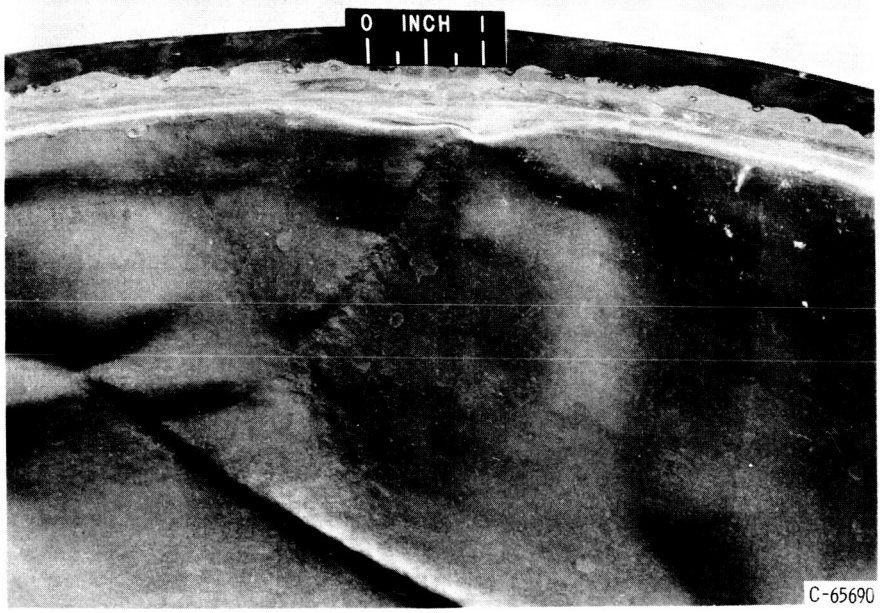

Figure 12. - Double fold at flange joint in diaphragm configuration C after completion of expulsion cycle, 0.016-inch-thick diaphragm (95 percent expulsion, test 7).

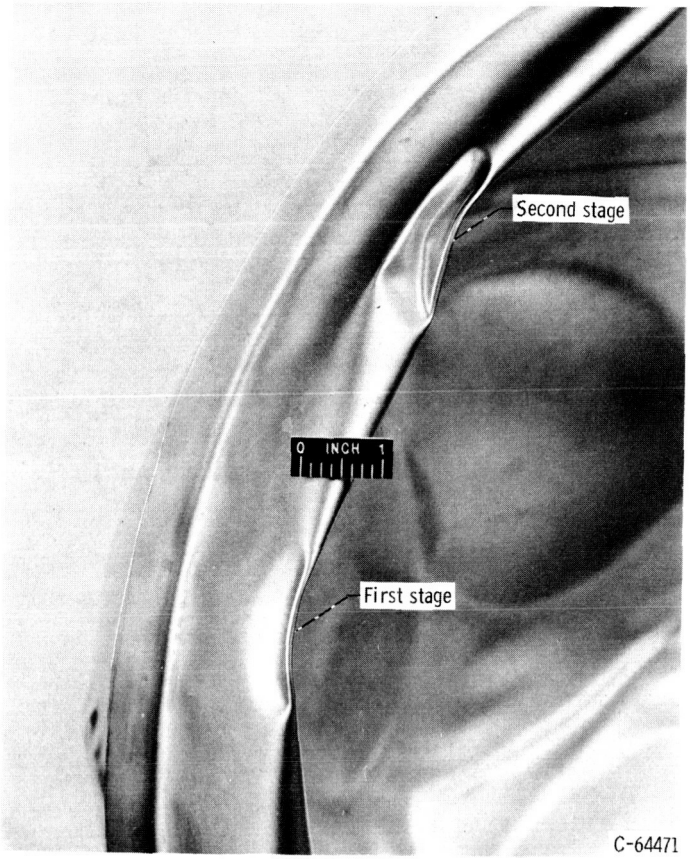

Figure 13. - Progressive stages of double folds in diaphragm. Configuration A; test 3.

and remained constant for most of the run. Deformation was fairly uniform, and where cornering occurred the radii of curvature were larger than the previous diaphragms. No leaks occurred during expulsion, and the test was arbitrarily stopped at about 95 percent expulsion so that the diaphragm could be examined intact. Only two double folds, much fewer than observed previously in configuration A and B type diaphragms had formed, but neither had torn. These folds (figs. 11 and 12) were much shallower than in previous tests, as can be seen from the comparison with figures 13 and 14, and are less likely to tear. An expulsion of 95.6 percent was attained that could have been improved if the test were continued.

Test 8, Configuration C, 0.016-Inch Wall Thickness

The eighth expulsion test again used configuration C. This test was conducted to check the cycle life of the diaphragm. The weight of the water, in this case, removed the indentation in the diaphragm while the containment sphere was being filled, giving the diaphragm a spherical dome. Maximum flow (490 to 500 lb/hr), limited by line sizes, was used in the test. The completely spherical dome gave the diaphragm more initial strength than in previously tested diaphragms, and a higher initial deformation pressure was required. Deformation started at approximately 9 pounds per square inch and the pressure immediately dropped to 2.40 pounds per square inch. The test was arbitrarily stopped when the Heise gage used to measure P_2 (see fig. 1, p. 2) reached the end of its range (15 psi). At this point, deformation consisted only of stretching the material to remove the wrinkles, and it was not considered important to continue the test. An expulsion of 98.3 percent without leakage was attained and this could have been improved if the applied pressure was allowed to exceed 15 pounds per square inch. The diaphragm was removed for inspection and photographing. It was then replaced in the containment sphere, and a recycling attempt was made. Failure occurred at approximately 20 percent reverse expulsion and seemed to be the result of a low cycle fatigue failure rather than a double-fold-type failure.

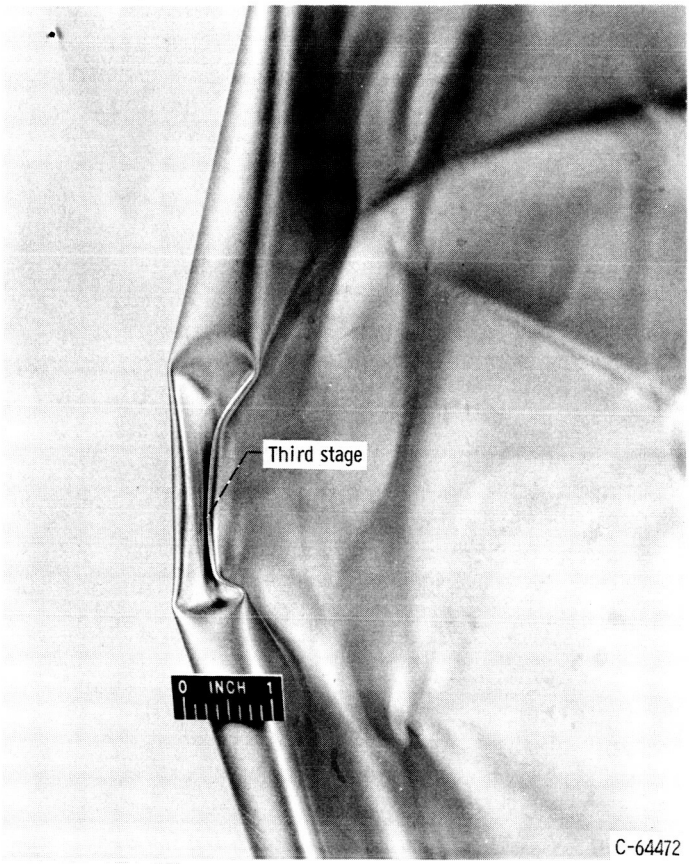

Figure 14. - Fully formed double fold in diaphragm. Configuration A; test 3.

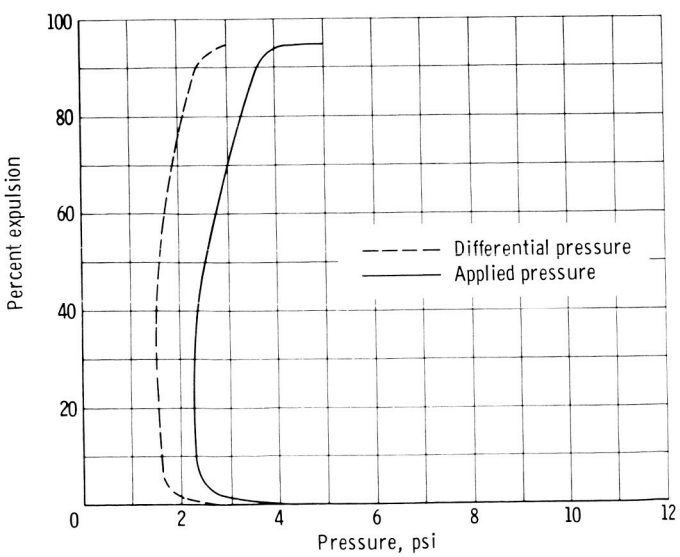

Figure 15. - Typical percent expulsion against pressure.

Pressure and Deformation Characteristics

The pressure and deformation characteristics of the diaphragm can be discussed in a general manner since all the diaphragms performed similarly in this respect. A curve of percent expulsion plotted against applied and differential pressure, which was typical for all the diaphragms tested is shown in figure 15. After the initial deformation, the applied pressure decreased rapidly during the first 2 percent expulsion. The deformed area was increasing at a rate such that the load per lineal inch on the perimeter of the deformed surface was nearly constant with the decrease in applied pressure. Typical deformation up to this point would appear as in figure 7(a). The arch-type bulges formed during deformation give strength to the diaphragm and when one of these buckled (at approximately 5 percent expulsion), a sharp pressure drop resulted. Decreased structural strength and the larger deformed area allowed the diaphragm to deform at an increased rate, thus increasing the flow rate. Typical deformation at this point would appear as it does in figure 7(b) (p. 7). Deformation continued at essentially constant pressure until approximately 40 percent expulsion, when the factor of increased force necessary to roll the material over itself overcame the increase in deformation area and the applied pressure began to increase. As shown in the curve of figure 15, this gradual increase in pressure continued until approximately 95 percent expulsion, if failure did not occur. Beyond approximately 95 percent expulsion, a

rapid increase in pressure was noted (accompanied by a decrease in volume flow) and was the result of the increased pressure required to stretch the material to remove the wrinkles formed during deformation. The difference between the applied and differential pressure curve is due to pressure drop in the lines.

DISCUSSION

The walls of a metal diaphragm are relatively thin and will buckle under small external pressures. This is a desirable characteristic since it minimizes the differential pressure needed to deform the diaphragm. When deformation first starts, the buckling waves are large, but as the diaphragm collapses, the bend radii decrease and double folds can occur. Double fold formation is similar to the buckling of thin-walled cylinders under compression. These double folds occur at localized points in the diaphragm. Figures 13 and 14 show progressive stages in double fold formation. These photographs were taken of a single diaphragm after it had been used in an expulsion test. Manner of development and severity of a double fold is dependent on the contour of the diaphragm. The severity of the bend (as measured by the bend radius), sheet thickness, and material physical properties govern the magnitude of the strain.

Failure of a diaphragm occurs when a hole or crack develops in the sheet metal due to local fracture. In a diaphragm that will be cycled, failure will occur by fatigue because of repeated folding on the same lines. Fatigue failure can be predicted by data obtained from strain cycle tests. An experimental curve for the variation of minimum required ductility with the number of folding cycles and bend radii is given in reference 1. For 304 stainless steel with a maximum percent reduction by cold working of 70 percent, a diaphragm can be expected to sustain between 1 and 2 cycles at ambient temperature before fatigue failure, assuming zero bend radius as in the case of a double fold. A cyclic test of diaphragm configuration C (test 8) produced approximately 1.2 cycles before fatigue failure. The problem in metallic diaphragms seems to be the minimizing of double folding or more specifically, eliminating zero bend radii.

Theoretical buckling loads for spherical shells under external loading can be calculated based on Love's equations. For a complete hemisphere if the buckling stress $\sigma_{cr} = P_{cr}R/2t$ (where P_{cr} is the critical buckling pressure, R is the radius of the sphere, and t is the thickness), then in terms of material properties

$$\sigma_{cr} = \frac{\frac{ET}{R}}{\sqrt{3(1 - \gamma^2)}}$$

where E is Young's modulus (28×10^6 psi for 304 stainless steel) and γ is Poisson's ratio (0.285 for 304 stainless steel). For a 0.016-inch diaphragm P_{cr} = 71.3 pounds per square inch, while for a 0.010-inch diaphragm P_{cr} = 27.9 pounds per square inch. Experimental buckling values have been found to be approximately one-fourth of the theoretical values (ref. 5). From the data of

these tests, denting the dome of the hemisphere seems to lower the buckling values to approximately one-twentieth of the theoretical values. It was found in test 8, in which the dome had been reformed to that of a hemisphere, that the buckling pressure increased to one-eighth of the theoretical values. The material where the dome had first been dented had been weakened or the buckling pressure would have been still higher.

Various random buckling and deformation patterns introduced undesirable increases in diaphragm stiffness with a possible reduction in percent expulsion for a given working pressure. This increased stiffness was apparent from the increased pressure differential required as deformation proceeded. Controlled folding of the diaphragm would be desirable, and there are several ways in which this might be done. Scoring the metal (over-stressing in a localized region) could help control bending and thus minimize tearing. Chemical milling to vary the thickness of the metal could also be used to make stresses more uniform. Reinforcing rings could also be used in the highly stressed regions. An exact analysis would be necessary to determine where the most highly stressed areas were and how to best use any solution. Controlled deformation would then be possible and both cornering and double folding might be eliminated.

Single and multiple folds and their random formations are an inherent characteristic of a collapsing bladder configuration. Double-fold-type failures are not normally encountered in ordinary applications of metals. Generally this type of failure mode occurs when materials are used in a foil- or film-type application.

An expulsion diaphragm should be designed so that during the expulsion cycle, folding or doubling back of the material is avoided. This was done in this investigation by eliminating the regions within the diaphragm where 180° folds were necessary.

The possibility of performing a mathematical study of the design parameters, with the purpose of calculating the strength and other requirements of the diaphragm as well as a basis for determining an optimum design, was considered. It was obvious that the unknown quantities involved made a purely mathematical analysis impossible. The difficulty in analyzing the behavior of a diaphragm during its expulsion cycle was due to the problem of synthesizing the deflection and collapse of shells in which local yielding was exceeded. Unpredictable wrinkles, creases, and folds resist the deformation of the diaphragm and add complexity to analytical design solutions. In conventional shell design, initial buckling is considered failure, but for an expulsion diaphragm, the initial buckling and deformation must be extended to complete collapse. Assumptions can be made regarding movement of a section, but investigation on this basis was beyond the scope of this program.

The advantages of this metallic diaphragm for the application considered are as follows:

(1) It is applicable over the flow range tested (150 to 500 lb/hr).

(2) It can be used over a large range of system pressure levels.

(3) The pressure differential needed during the greater portion of the expulsion cycle is small, producing a low energy requirement system.

(4) Fabrication of the diaphragm and system operation are simplified.

(5) It is lightweight because of the efficiency of its configuration and method of expulsion.

The disadvantages are as follows:

(1) Compatibility requirements limit the material selection.

(2) Replacement of the diaphragm, although relatively simple, requires dismantling of the containment tank and removal from the missile if it was previously installed.

(3) By nature, this is a "one-shot" device requiring replacement prior to each subsequent cycle.

These last two are only disadvantages for test purposes; in actual one-shot flight operation, no replacement would be necessary. The requirements for one-shot operations are less stringent than for repeated cycles since some damage to the diaphragm can be tolerated without adverse results during the expulsion cycle. Only testing under closely simulated flight conditions can be expected to render the information necessary for final evaluation of the diaphragm design.

SUMMARY OF RESULTS

The results of investigating hemispherically shaped metallic expulsion diaphragms made from type 304 stainless steel using water as the working fluid indicated the following:

1. Greater than 98 percent expulsion without failure was obtained only with diaphragms having a configuration that was less than a complete hemisphere. In this investigation a diaphragm with a 1/2-inch equatorial segment removed from a full 22-inch-diameter hemisphere achieved successfully 95 to 98 percent expulsion.

2. Diaphragms whose configurations were slightly more than a full hemisphere failed by pin-holing or tearing, resulting in a leak through the diaphragm after only 60 to 82 percent expulsion was obtained. Failure occurred in the region where approximately 180° folding was necessitated.

3. Reducing the diaphragm wall thickness from 16 to 10 mils had a detrimental effect. For the same configuration operated at a similar flow rate a 0.016-inch-thick diaphragm failed at 82.1 percent expulsion while a 0.010-inch-thick diaphragm failed at 68.5 percent expulsion.

4. The use of spun convolutions in the region where failure occurred did

not improve the percent expulsion.

5. It appears that metallic diaphragms without controlled deformation cannot obtain more than one complete expulsion cycle without failure. An attempt to make a second expulsion cycle using a diaphragm that had successfully completed 1 cycle resulted in a fatigue failure after approximately 20 percent expulsion.

6. An indentation in the dome of the diaphragm aided deformation and significantly lowered the initial buckling pressure. Unsymmetrical deformation of the diaphragm did not seem to affect the percent expulsion.

Lewis Research Center,
National Aeronautics and Space Administration,
Cleveland, Ohio, April 6, 1965.

REFERENCES

1. Krivetsky, Alexander; Bauer, William H.; Loucks, Harvey L.; Padlog, Joseph; Robinson, John U.; and Walters, William H.: Research on Zero Gravity Expulsion Techniques. Rept. No. 7129-933003, Bell Aerosystems Co., Mar. 1962.

2. Cassidy, F. H.; Kaelin, W. H.; Keeler, M. J.; and Knoll, E. F.: Flexible Expulsion Bladder Design Study. Rept. No. 1082, Aerojet-General Corp., Mar. 16, 1956.

3. Bell, J. E.; Killian, W. R.; Penner, J. E.; Hope, D. H.; Sutton, H. E.; and Tweed, R. M.: Development of Positive Expulsion Systems for Cryogenic Fluids. Rept. No. 13511 (SSD-TDR-62-14), Phases 2-3, Beech Aircraft Corp., May 1962.

4. Sirocky, Paul J.: Transfer of Cryogenic Fluids by an Expulsion-Bag Technique. NASA TN D-849, 1961.

5. Goerner, Erich: Buckling Characteristics of Spherical or Spherically-Dished Shells. Rept. No. 1R9, Army Ballistic Missile Agency, Feb. 6, 1956.